



ZAG

ZAVOD ZA
GRADBENIŠTVO
SLOVENIJE

SLOVENIAN
NATIONAL BUILDING
AND CIVIL ENGINEERING
INSTITUTE



UNIVERSITY
OF LJUBLJANA

FGG

Faculty of Civil and
Geodetic Engineering

Using Bridge Weigh-in-Motion System for Structural Health Monitoring of Bridges

ISWIM Young Researcher Award Webinar

Doron Hekič MEng (Civil)

ZAG Slovenian National Building and Civil Engineering institute

28. 8. 2025



Content

- Introduction
- Literature review and terminology
- Theory background
- Case study
 - Calibration vehicle passages
 - Extraction of B-WIM influence line
 - Acceleration measurements
 - FEMU
 - Validation
- Conclusions

Ageing infrastructure

- Six European countries, 2011: 85% older than 35 years
- Slovenia, 2017: ≈ 60% older than 50 years (non highway roads)
- Germany, 2022: > 50% older than 40 years
- United States, 2021: average age of bridge is 44 years
- United States, 2025: average age of bridge is 47 years

Increasing traffic loads

- Total transport activity increase 2019 – 2050:

≈ 79 %
Passenger
transport



≈ 100 %
Freight
transport



Increasing extreme weather events

- Scour is the number one cause of bridge failures:
 - In most countries
 - Reported:
 - In United States (Briaud et al. (2014))
 - In Italy (D'Angelo et al. (2025))

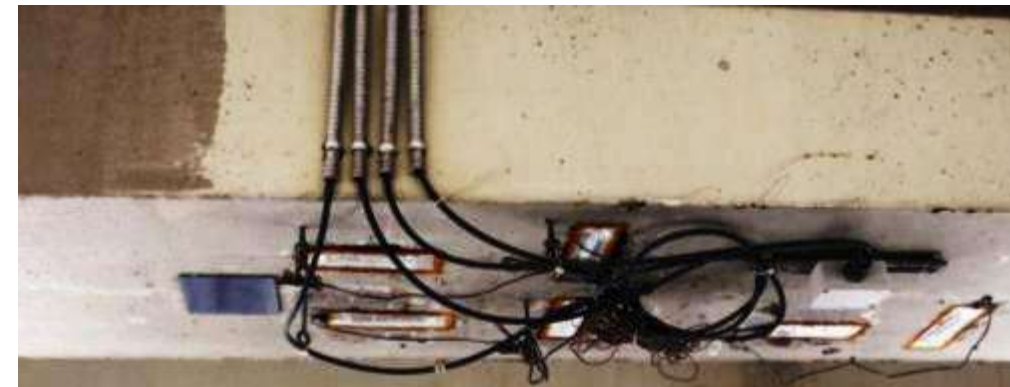
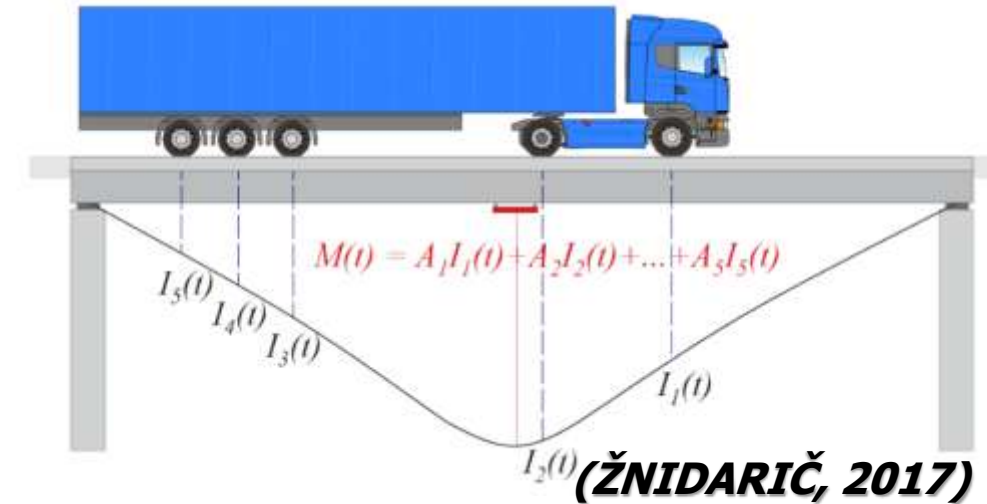


Urgent need for more advanced and continuous monitoring techniques

- Recognised more than 20 years ago (Chang et al. 2023)
- Traditional inspection/assessment techniques are irreplaceable, but are:
 - Expensive
 - Labour intensive
 - Rare (1 x every 3 years, every second inspection is principal inspection)
- Goal is to have a system that enables earlier detection of structural issues and more informed maintenance decisions

Literature review: terminology

- Bridge weigh-in-motion (B-WIM)
 - A specific weigh-in-motion technique that uses an instrumented bridge or culvert to weigh the passing vehicles at highway speed (Žnidarič, 2017)
- Structural health monitoring (SHM)
 - Integration of sensing and possibly also actuation devices to allow the loading and damaging conditions of a structure to be recorded, analyzed, localized, and predicted in a way that nondestructive testing (NDT) becomes an integral part of the structure and a material.” (Boller, 2009)
 - Process of implementation of a damage detection strategy (of civil engineering structures) (Farrar & Worden, 2012)



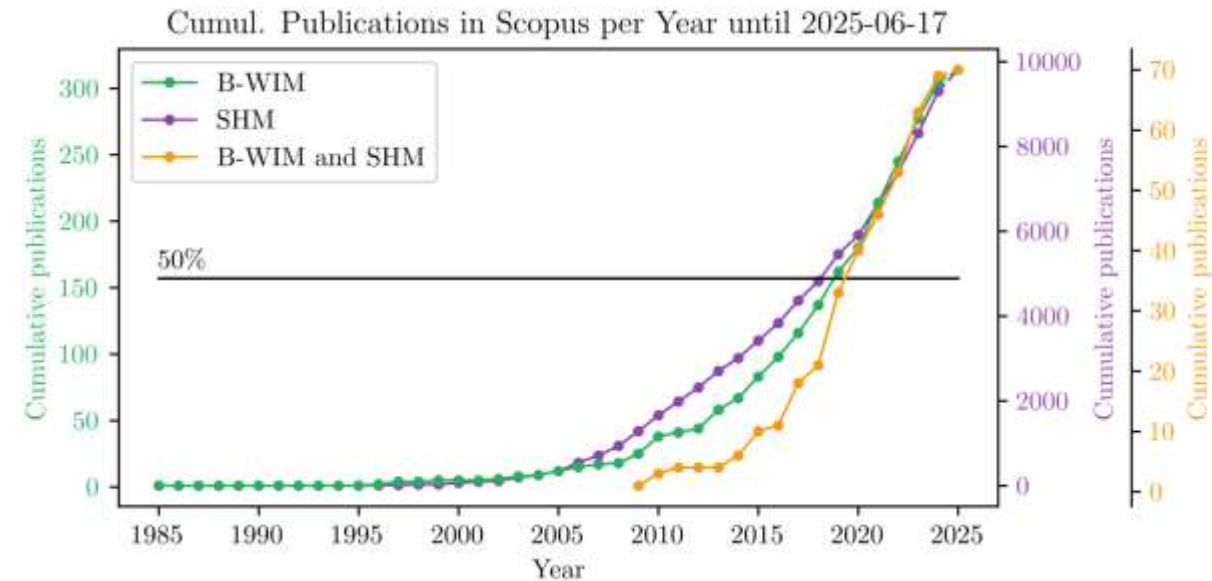
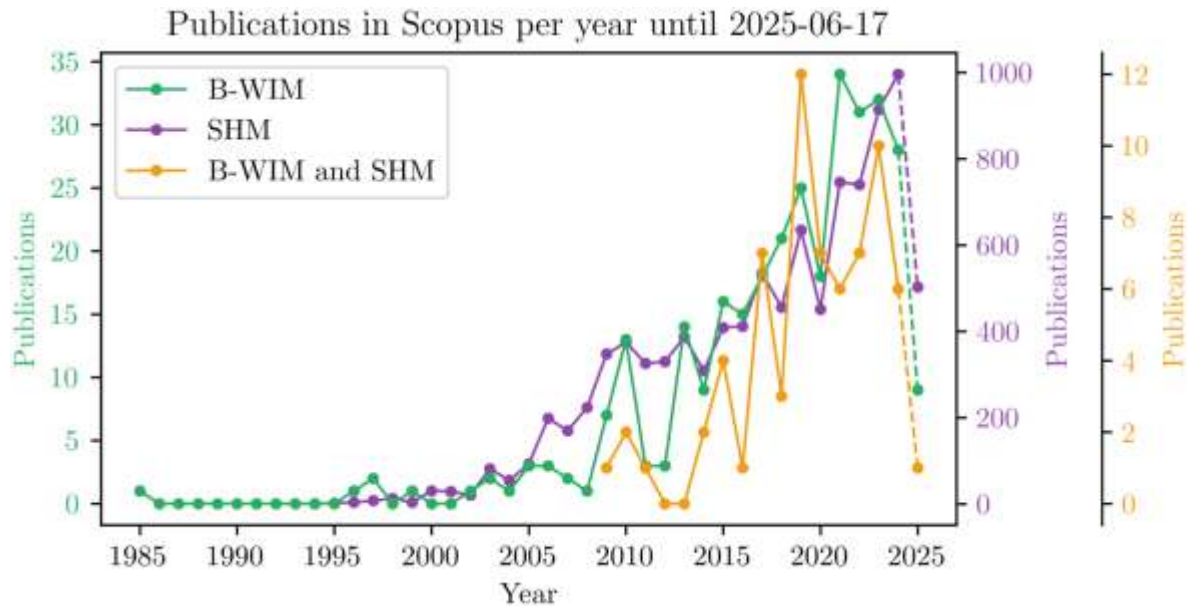
Finite element model updating (FEMU) - why?

- Finite element model updating (FEMU)
 - FEMU is a specific technique often used within SHM to update the FE model of a structure so that it accurately reflects the current (possibly damaged) state of the real structure (Ereiz et al. 2022).
- Safety analyses
 - When performing safety analyses of existing bridges it is crucial to have the realistic representation of the real structure (original design documentation is not enough)
- Damage detection
 - SHM → model-driven vs. data-driven approach



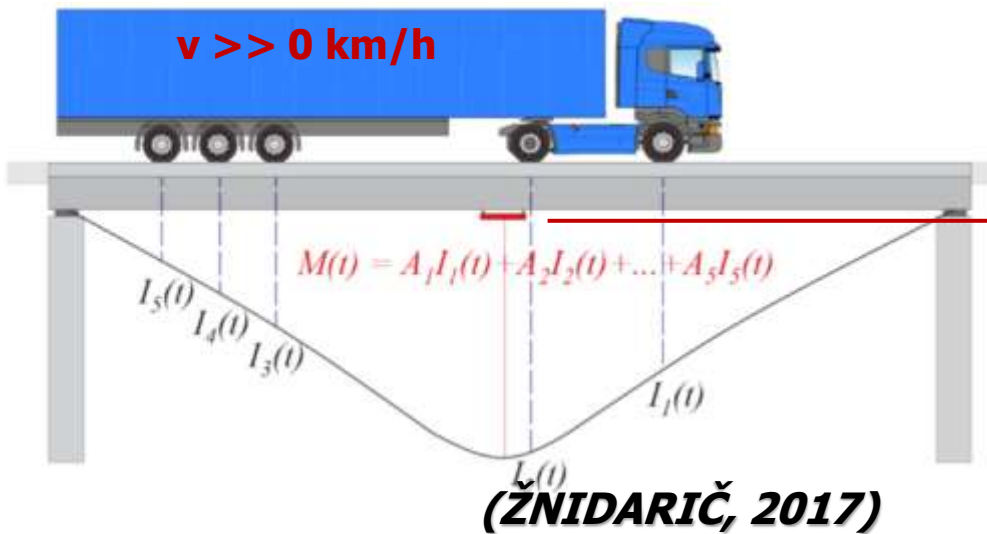
Literature review: Scopus database for B-WIM, SHM, B-WIM & SHM

- Most of the B-WIM and SHM literature was published in last 6-7 years
- First B-WIM & SHM study was published (Scopus) in 2009

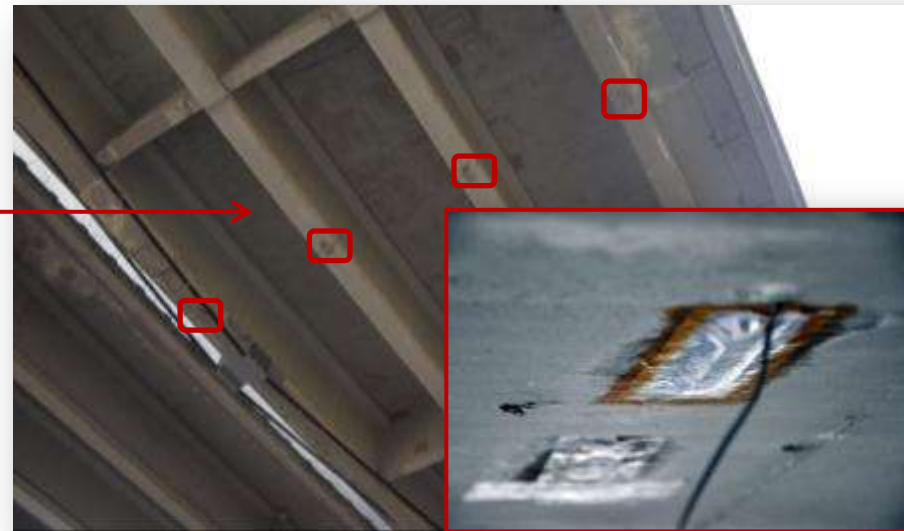


Theory background: B-WIM

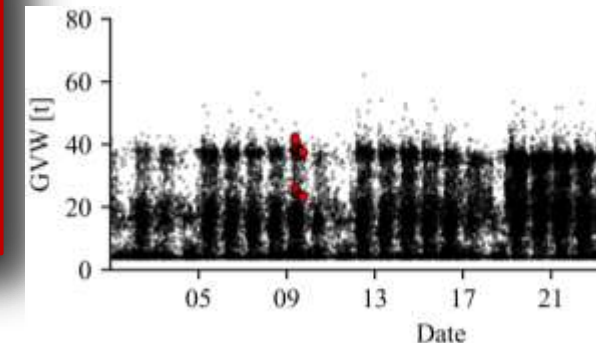
- Core assumptions still valid from Moses (1979) : Bridge oscillates around a static equilibrium position during vehicle passage, Bernoulli's plane sections, linear stress-strain relationship
- Needs calibration with truck(s) of known weight



$$M(t_j) = \sum_{i=1}^N A_i I(x) = \sum_{i=1}^N A_i I(v(t_j - t_i)); j = 1 \dots N_M$$

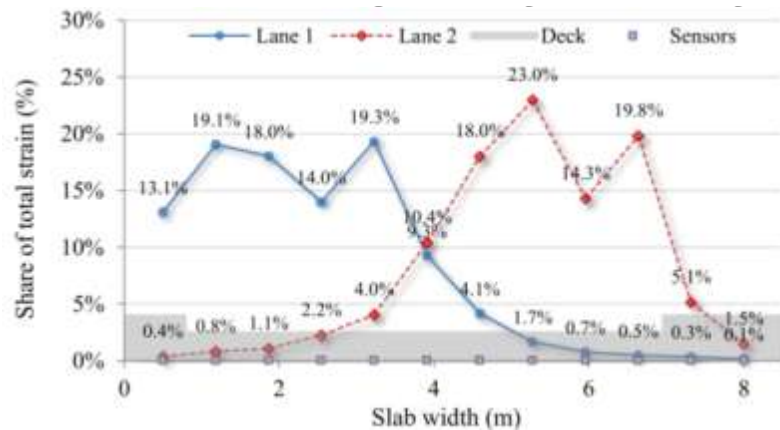


axle weights,
axle distances,
velocities

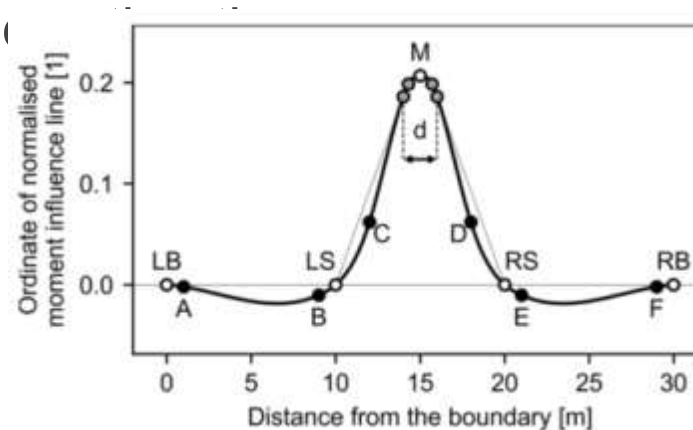


Theory background: B-WIM

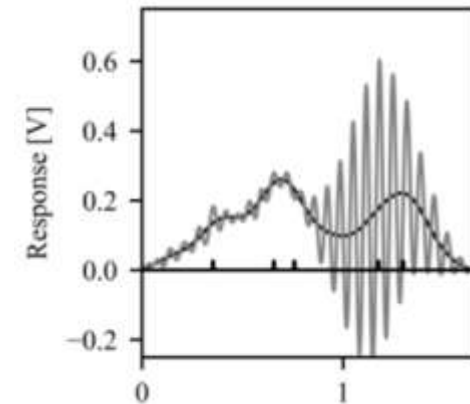
- Beside axle loads, other features can also be obtained from B-WIM system:
 - Load (girder) distribution factors
 - Influence Line
 - Dynamic Amplification Factor (DAF)



(ŽNIDARIČ, 2017)



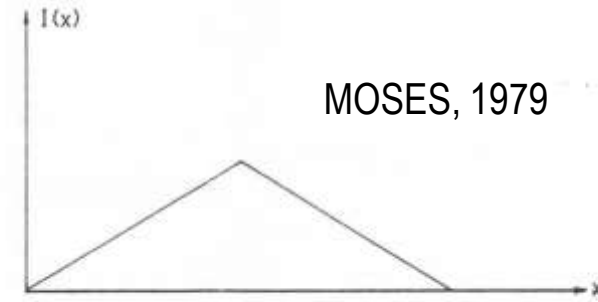
(ŽNIDARIČ & KALIN, 2020)



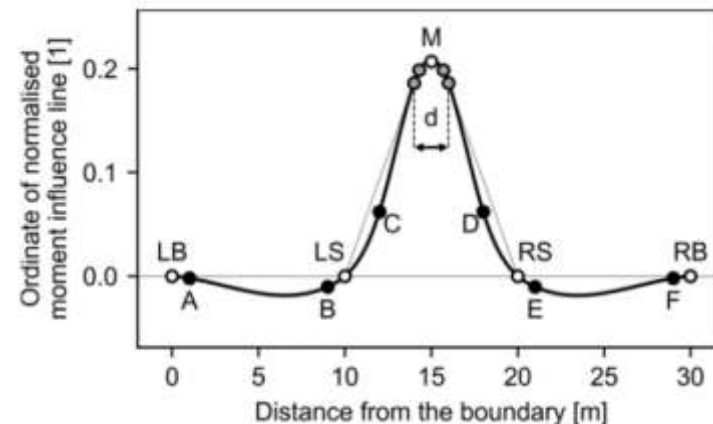
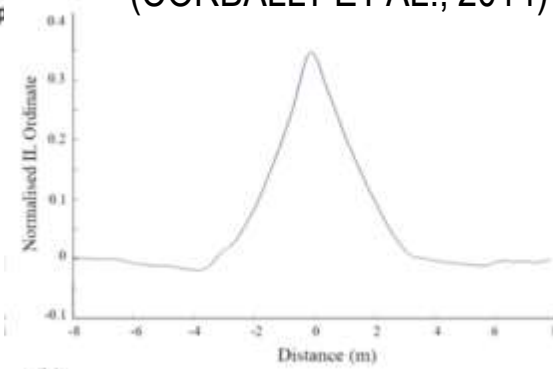
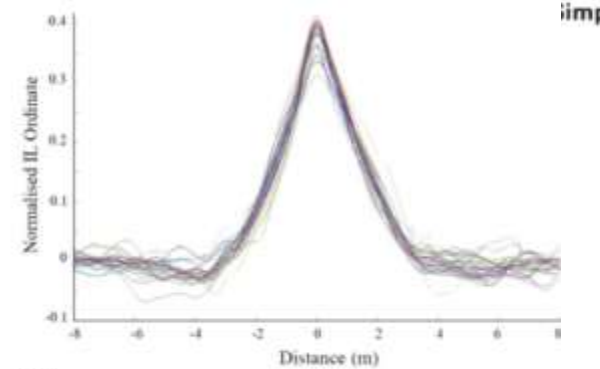
(KALIN ET AL., 2021)

Theory background: B-WIM

- In the beginning of the B-WIM, the theoretical influence lines were used. Simply supported girder example → ideal triangular-shaped influence line.
- In 2000s, theoretical influence lines were replaced for measured ones (matrix method, ZAG method)
- In 2017, 2020 the parametrised ZAG method was introduced
- ZAG method employs non-linear optimisation and utilises a large number of randomly selected vehicles from regular traffic, whose axle loads are unknown, to estimate the influence line shape.
- To derive the ZAG influence line, same equation is used as for the weighing, with additional parameters that describe the shape of the influence line.
- Slight modification of the ZAG influence line had to be done, because the original ZAG method normalises the influence line such that the area under influence line is 1



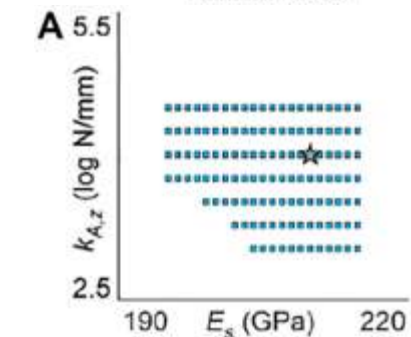
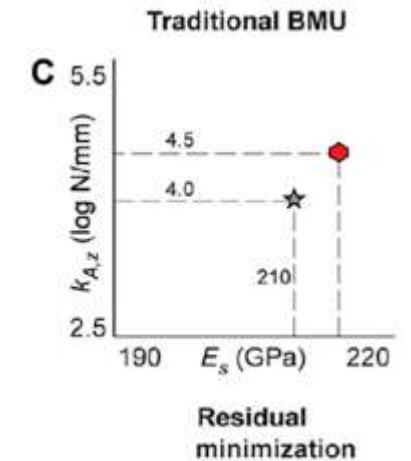
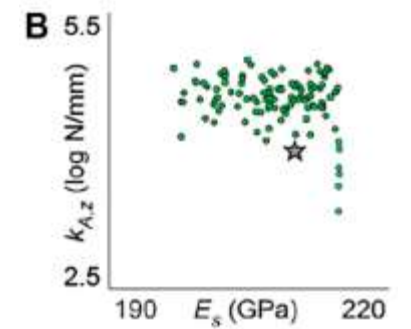
(MCNULTY ET AL., 1999)
(OBRIEN ET AL., 2005)
(CORBALLY ET AL., 2014)



(ŽNIDARIČ, 2017)
(ŽNIDARIČ & KALIN, 2020)

Theory background: FEMU

- The FEMU problem is defined as the difference between the structural behaviour predicted by the FE model and the actual (measured) behaviour.
 - Iterative stochastic FEMU → statistical problem
 - Bayesian interference
 - Iterative deterministic FEMU → optimisation problem)
 - FEMU is performed using the maximum likelihood method (MLM)
 - Single-objective (used in this PhD) and multi-objective optimisations
 - Manual FEMU → trial and error approach
 - Automatic FEMU → nonlinear optimisation using various algorithms:
 - Sequential least squares programming (SLSQP)
 - Particle swarm optimisation (PSO)
 - Genetic algorithm (GA)
 - Error-domain model falsification (EDMF) → gaining attention in recent years (used in the PhD)
 - Karl Popper's concept from 1930's
 - Models cannot be fully validated by data, they can only be falsified



- EDMF CMS samples
- Traditional BMU samples
- Residual minimization solution
- True values of model parameters

PAI & SMITH (2022)

Theory background: FEMU

- Residual minimisation
 - Most authors minimise the difference of dynamic data:
 - **Natural frequencies** (most often)
 - **Mode shapes** through modal assurance criterion (MAC) (often)
 - **Combination** of natural frequencies and mode shapes (less often)
- Studies considering static data sets (**strains, displacements**) are rare
- Few studies combine static and dynamic data sets

$$J_f = \sum_{i=1}^n (f_{i,\text{nu}}^{\text{m}} - f_{i,\text{ex}}^{\text{p}})^2 \quad J_f = \sum_{i=1}^n \left(\frac{f_{i,\text{nu}}^{\text{m}} - f_{i,\text{ex}}^{\text{p}}}{f_{i,\text{ex}}^{\text{p}}} \right)^2$$

$$\text{MA}^{\text{C}}(\psi_{ci}, \psi_{di}) = \frac{|\{\psi_{ci}\}^T \{\psi_{di}^*\}|^2}{\{\psi_{ci}\}^T \{\psi_{ci}^*\} \{\psi_{di}\}^T \{\psi_{di}^*\}}$$

$$J_{\text{MA}^{\text{C}}} = \sum_{i=1}^n (1 - \text{MA}^{\text{C}}_i)^2$$

$$J_{f,\text{MA}^{\text{C}}} = w_f \cdot J_f + w_{\text{MA}^{\text{C}}} \cdot J_{\text{MA}^{\text{C}}}.$$

$$J_{\varepsilon} = \sum_{v=1}^{n_v} \sum_{g=1}^{n_g} \frac{(z_{\text{nu}}^{\text{m},v,g} - z_{\text{ex}}^{\text{p},v,g})^2}{\text{ST}_{\text{ex}^{\text{p},v,g}}^{\text{D}}^2}$$



ZAG

ZAVOD ZA
GRADBENIŠTVO
SLOVENIJE

SLOVENIAN
NATIONAL BUILDING
AND CIVIL ENGINEERING
INSTITUTE

CESTEL



DEWESoft[®]
measurement innovation

Model updating of bridges using measured influence lines

Goal:

- 1) Find out if it is possible to use B-WIM derived strain IL for FEMU and
- 2) how it performs compared to other, traditional (acceleration-based) FEMU

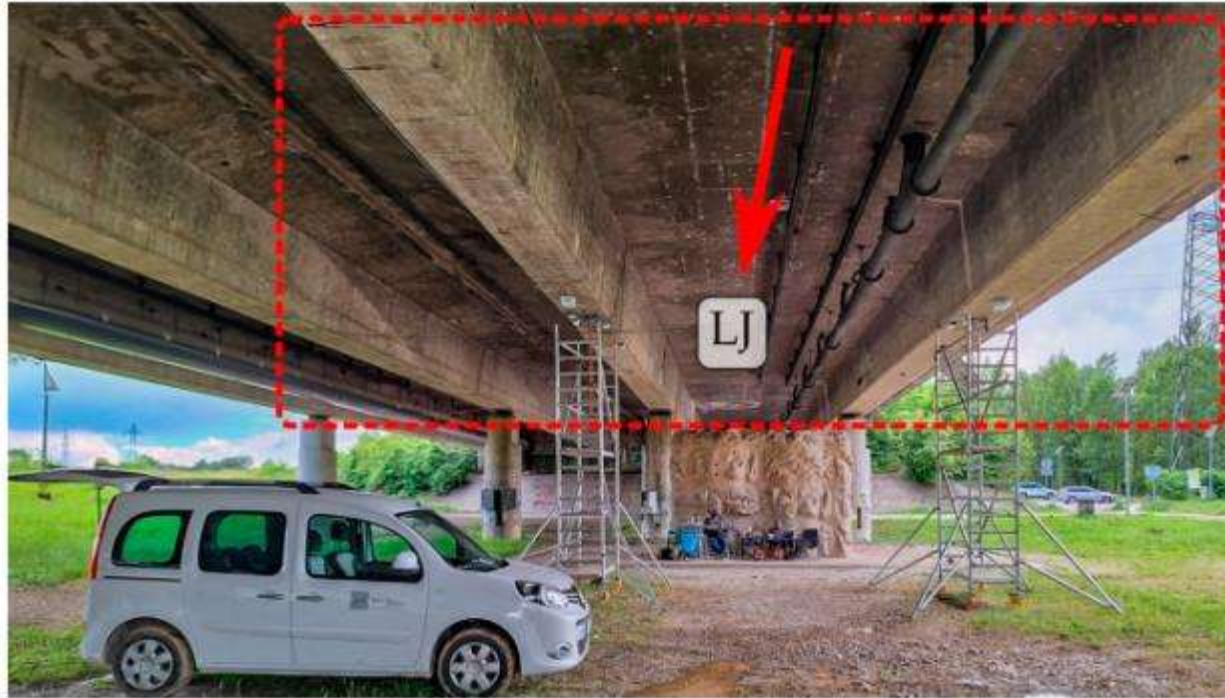
Aim:

Extending B-WIM towards SHM through usage of the B-WIM derived influence line for the FEMU

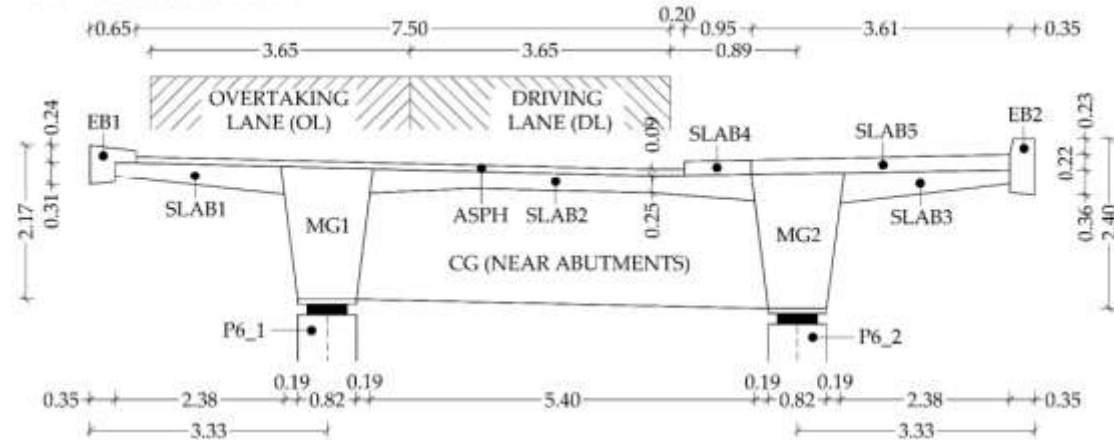
Case study viaduct

- Roadway bridge near Ljubljana (Tomačevo)
- Built in 1982
- 204 m long
- Seven-span continuous post-tensioned double-T section superstructure
- PC (superstructure)
- RC (support. structure)
- Crossing Sava river
- Two parallel structures
- Minor rehabilitation in 1990 and 2018
- Living-lab, under development from 2022

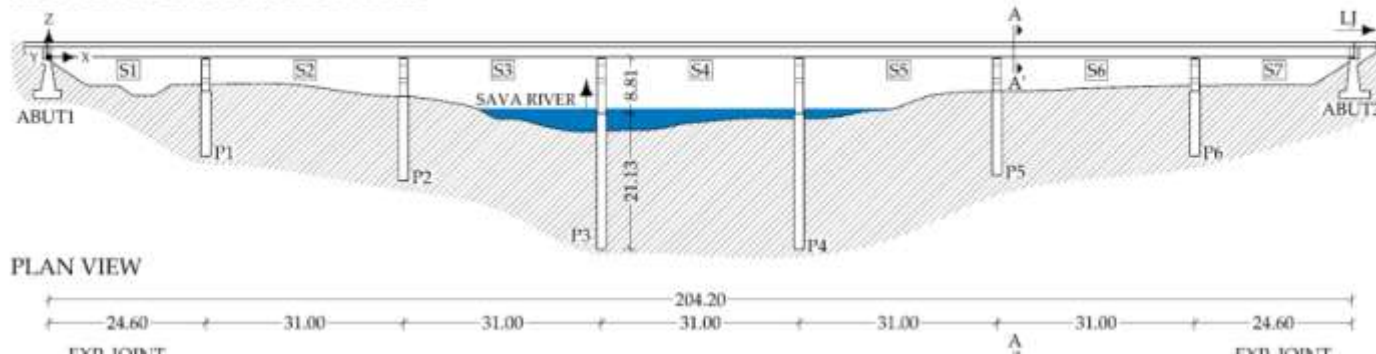
Case study viaduct



A-A' CROSS SECTION



SIDE VIEW ALONG UPSTREAM EDGE

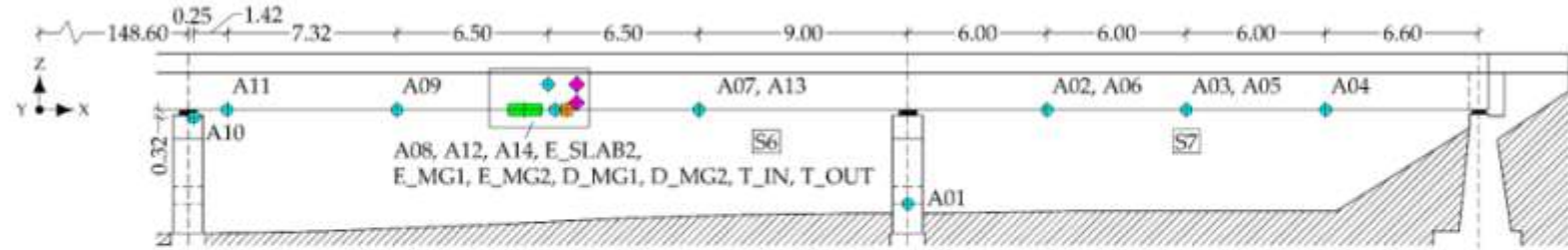


PLAN VIEW

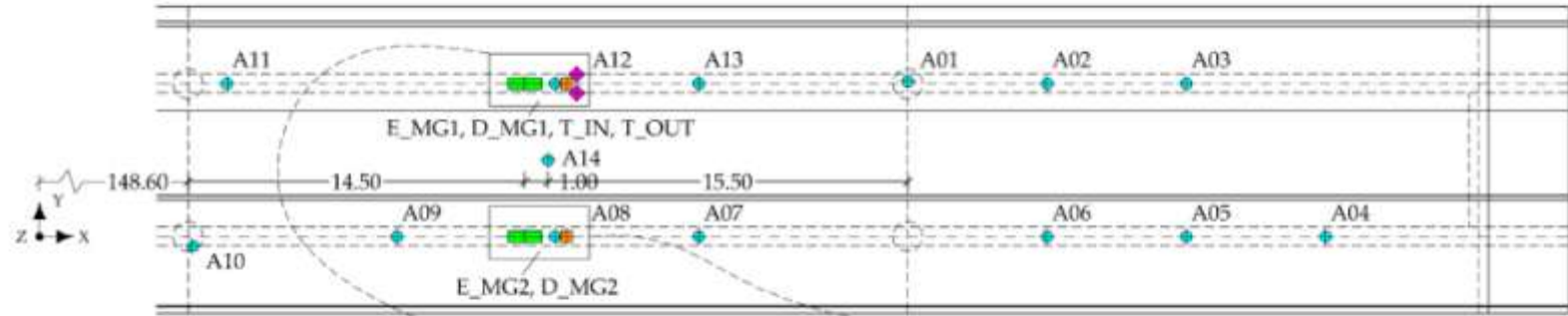
Measurements

- Sensors are installed in last two spans
- Sensors used for this study:
 - 14 accelerometers
 - 2 strain sensors (used for B-WIM), one on each girder's mid-span
 - 4 strain-based axle detectors (for B-WIM)
 - 2 displacement sensors
 - 2 temperature sensors
- 1st source of data: traffic induced strains and displacements
- 2nd source of data: modal parameters from ambient and traffic induced vibrations

SIDE VIEW ALONG UPSTREAM EDGE WITH SENSOR DISPOSITION: SPANS S6 & S7

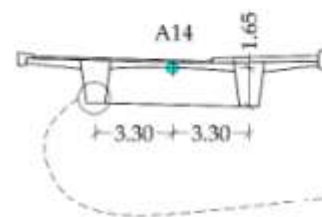


PLAN VIEW WITH SENSOR DISPOSITION: SPANS S6 & S7

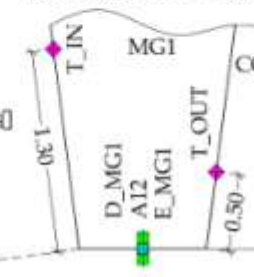


DETAILED VIEWS NEAR MID-SPAN

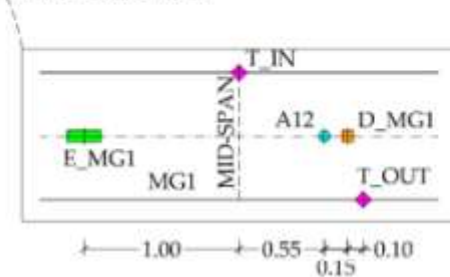
POSITION OF A14 IN CROSS-SECTION VIEW



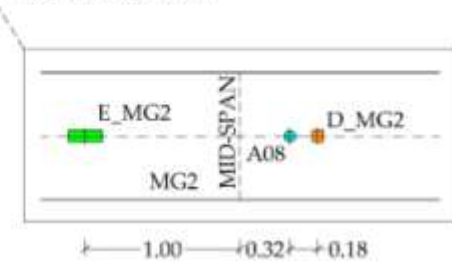
MG1: CROSS SECTION



MG1: PLAN VIEW



MG2: PLAN VIEW



Experimental campaign

Installation



Installation



Sensors



Static weighing



During measurements



During measurements



Calibration vehicle passages

- 2 different calibration vehicles
- Full on the 1st night, empty on the 2nd
- Overall 72 passages



(a)



(b)

Figure 7. Calibration vehicles: V1 (a) and V2 (b).

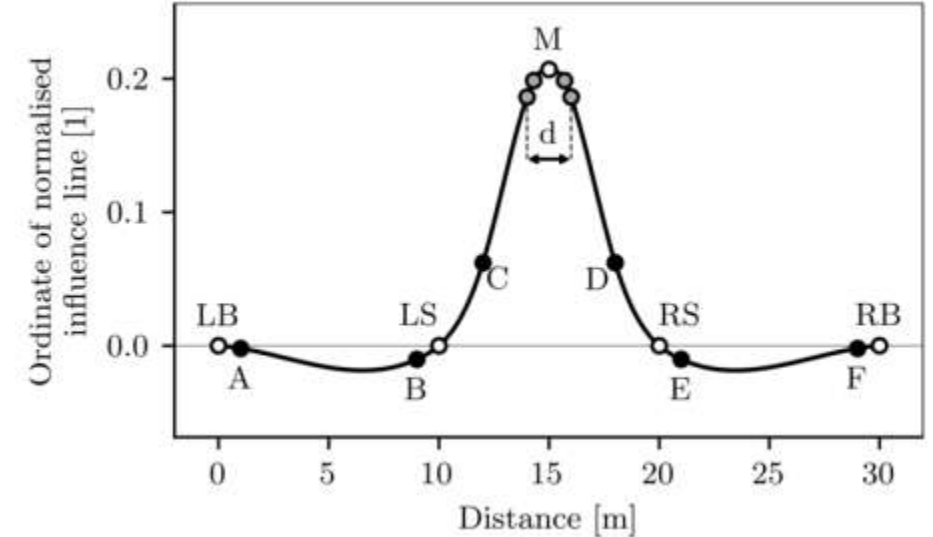
Table 1. Axle loads, axle spacing, and gross vehicle weights (GVW) of the calibration vehicles.

Vehicle ¹	1st Axle		2nd Axle		3rd Axle		4th Axle		5th Axle	
	Load (kN)	Spacing (m)	Load (kN)	Spacing (m)	Load (kN)	Spacing (m)	Load (kN)	Spacing (m)	Load (kN)	GVW (kN)
V1_F	68.67	3.42	73.58	1.37	71.61	/	/	/	/	213.86
V1_E	57.88	3.42	37.28	1.37	36.30	/	/	/	/	131.45
V2_F	69.65	3.60	90.25	2.82	64.75	1.31	61.80	1.31	59.84	346.29
V2_E	56.90	3.60	29.43	2.82	14.72	1.31	15.70	1.31	14.72	131.45

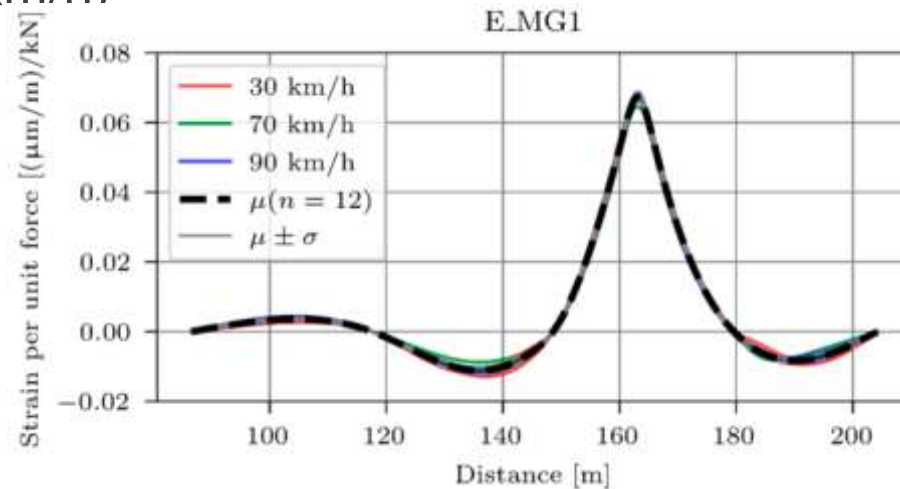
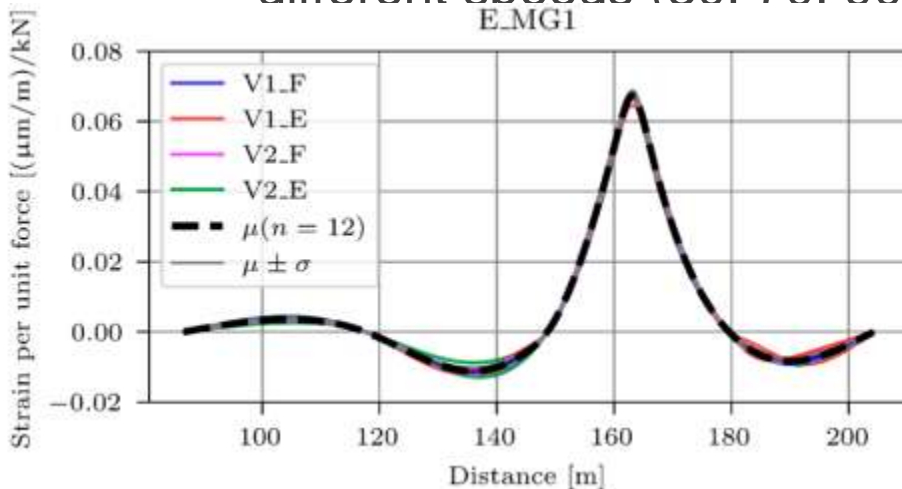
¹ F represents a fully loaded truck, and E an empty truck.

Extraction of the B-WIM influence line

- ZAG's method was used to extract the B-WIM influence line from the vehicle-induced mid-span strains.
- Modification was performed to replace normalised influence line for absolute.
- Influence of the following parameters on the influence line was investigated:
 - vehicle type (rigid vs. tractor with a semi-trailer)
 - load (loaded vs unloaded vehicles)
 - different speeds (30. 70. 90 km/h)

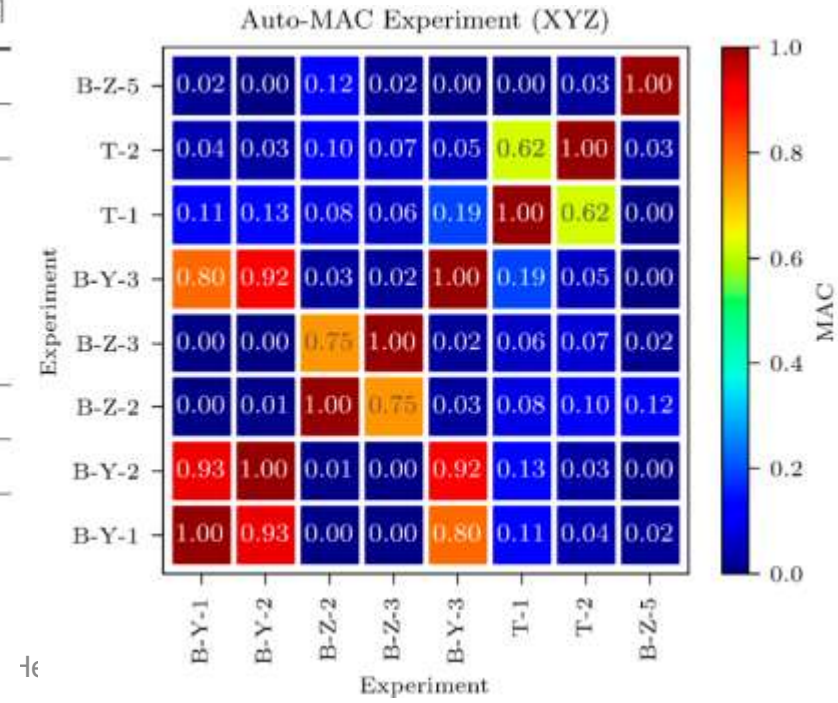
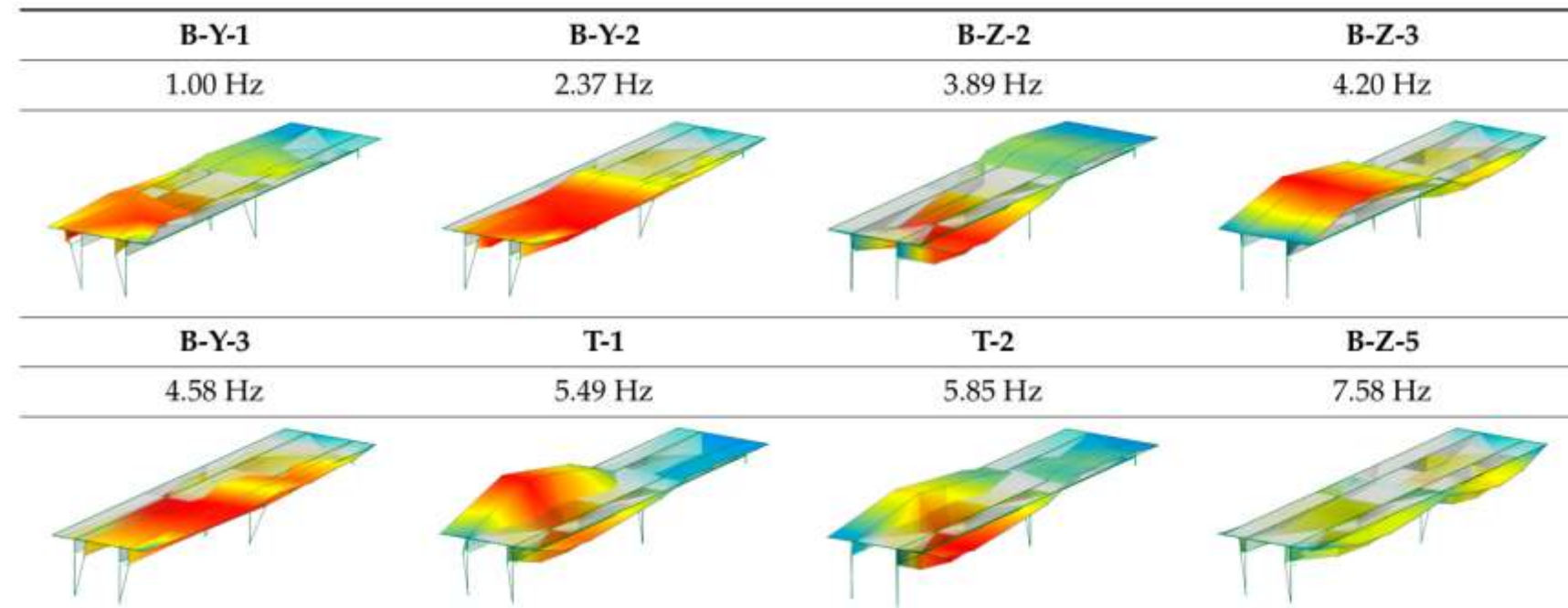
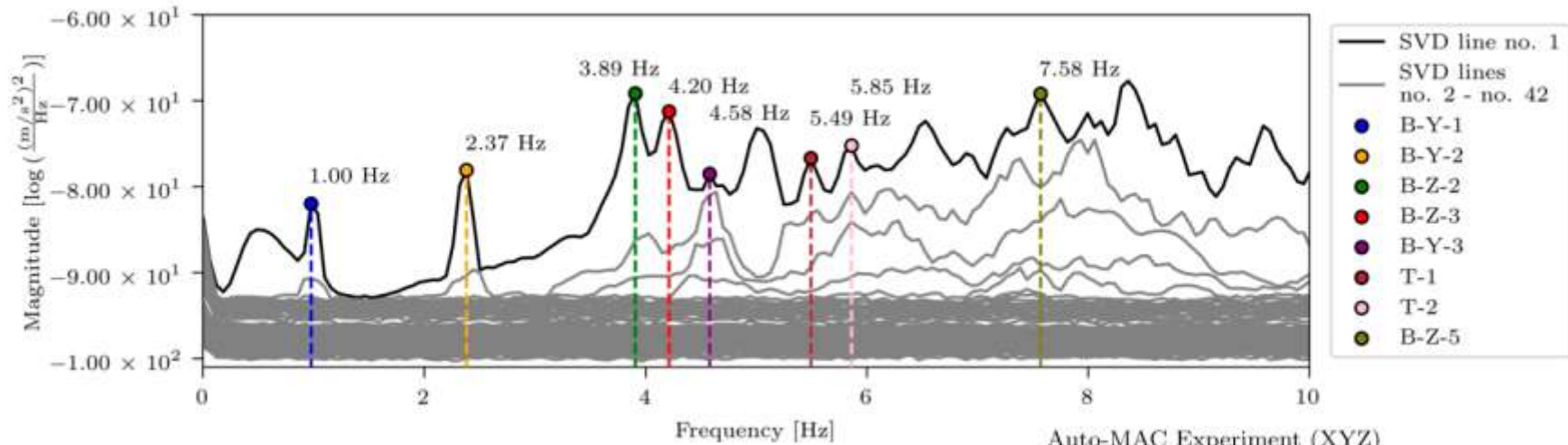


$$s(t_j) = \sum_{i=0}^N A_i I(v_i(t_j - t_i)); j = 1 \dots M$$



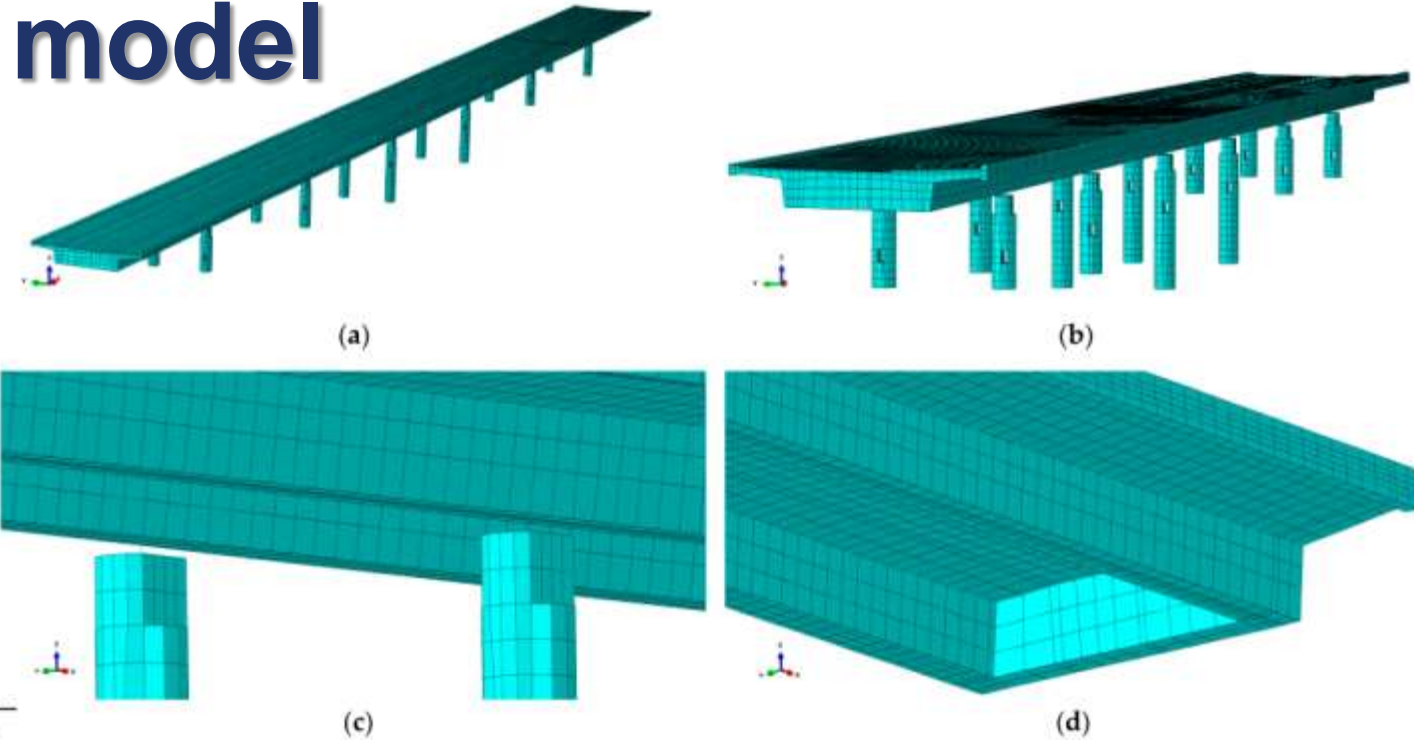
• Small deviation
 • Mean influence line for both strain-sensors were determined and

Ambient and traffic induced vibrations and extraction of modal parameters



Finite element (FE) model

- Seven spans (entire bridge)
- AutoCAD 3D solids → Abaqus CAE 2023
- C3D20R finite elements for superstructure
- C3D8R finite elements for the piers
- Elastomeric bearings → springs
- Properties from design documentation

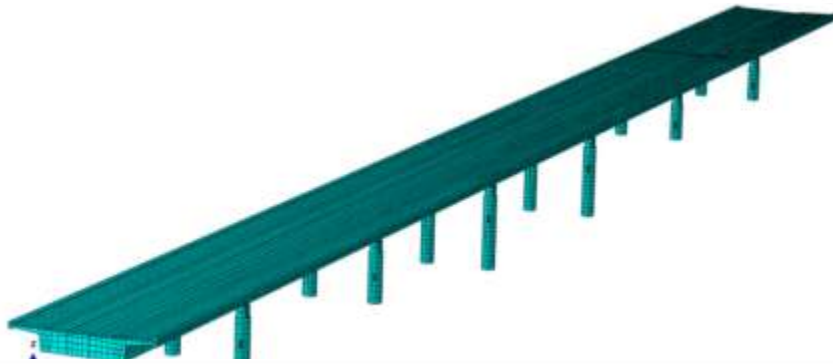
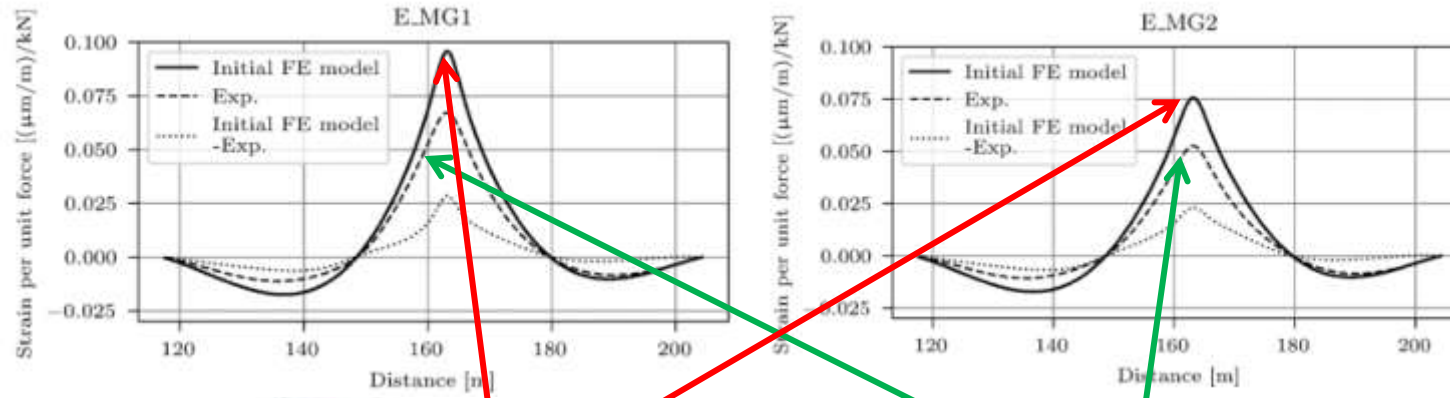


Element	Abbreviation	Young's Modulus (GPa)	Poisson Ratio	Density (t/m ³)
Asphalt	ASPH	8.00	0.35	2.582
Edge beam 1	EB1	31.00	0.20	2.710
Edge beam 2	EB2	31.00	0.20	2.580
Main girder 1	MG1	35.00	0.20	2.500
Main girder 2	MG2	35.00	0.20	2.500
Slab 1	SLAB1	35.00	0.20	2.500
Slab 2	SLAB2	35.00	0.20	2.500
Slab 3	SLAB3	35.00	0.20	2.500
Slab 4	SLAB4	35.00	0.20	3.573
Slab 5	SLAB5	14.59	0.20	1.177
Pier (bottom part) ¹	PIER_BOTTOM	31.00	0.20	2.500
Pier (upper part, bearing region) ¹	PIER_TOP	34.00	0.20	2.500
Cross girder	CG	35.00	0.20	2.500

Bearing	Position (Abutment, Pier)	Translational Stiffness (kN/m)		Vertical Stiffness (kN/m)	Rotational Stiffness (kNm)
		X Direction	Y Direction		
Elastomeric bearing type 1	P1, P6	3.18×10^3	3.18×10^3	1.77×10^6	3.41×10^4
Elastomeric bearing type 2	P2, P3	3.61×10^3	3.61×10^3	2.01×10^6	3.90×10^4
Elastomeric bearing type 3	P4, P5	4.19×10^3	4.19×10^3	2.33×10^6	4.55×10^4
Unidirectional pot bearing	ABUT1, ABUT2	Free	Rigid	Rigid	Free (0.01°)

¹ PIER_BOTTOM represents the bottom parts, and PIER_TOP represents the top parts (bearing region) of all pier pairs: P1, P2, P3, P4, P5, and P6.

FE model vs. measurements

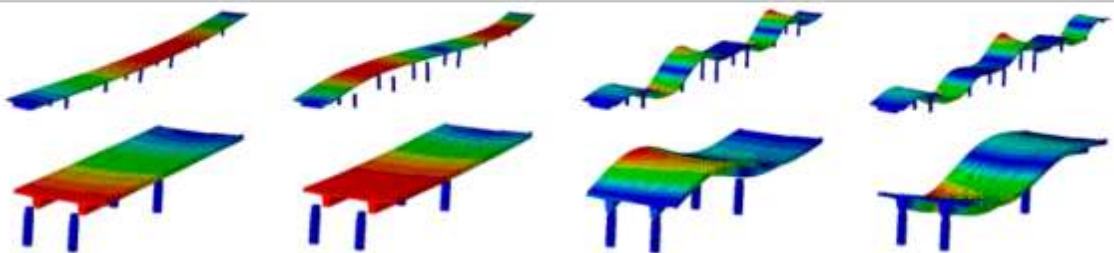


MODELLED

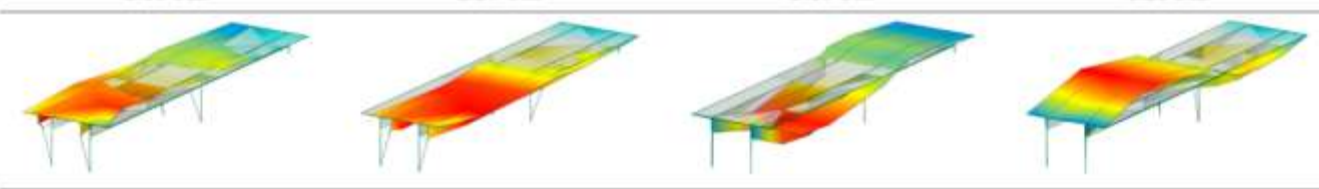
MEASURED



B-Y-1	B-Y-2	B-Z-2	B-Z-3
0.72 Hz	2.01 Hz	3.79 Hz	4.41 Hz



B-Y-1	B-Y-2	B-Z-2	B-Z-3
1.00 Hz	2.37 Hz	3.89 Hz	4.20 Hz



Sensitivity study

- Deterministic sensitivity study was performed to select the variables (parameters) to update
- 2 objective functions were defined to perform the sensitivity study

– Natural frequencies

$$J_f = \sum_{i=1}^n \left(\frac{f_{i,num} - f_{i,exp}}{f_{i,exp}} \right)^2$$

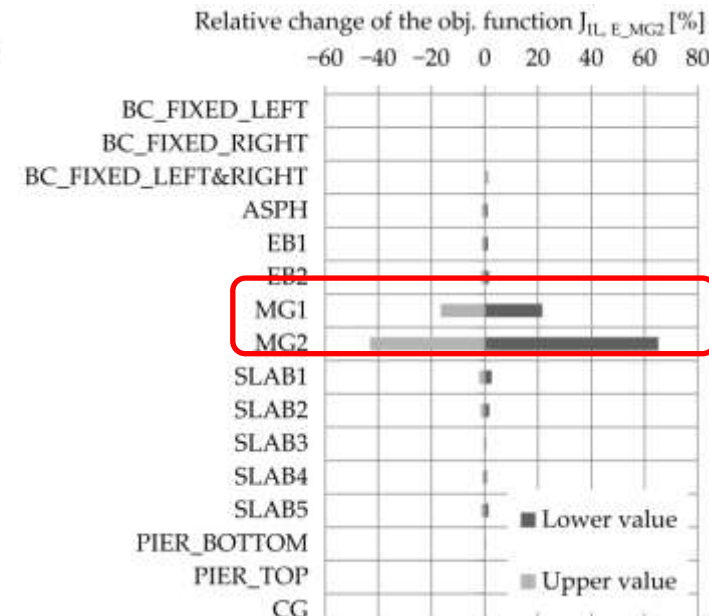
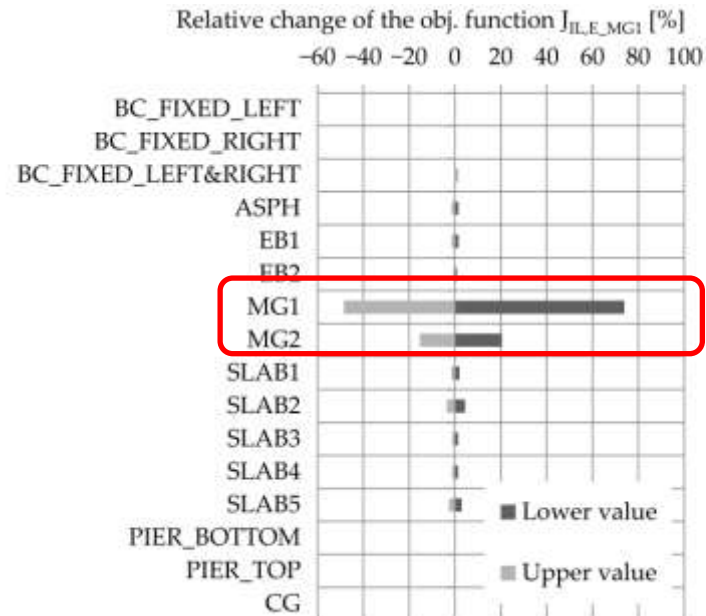
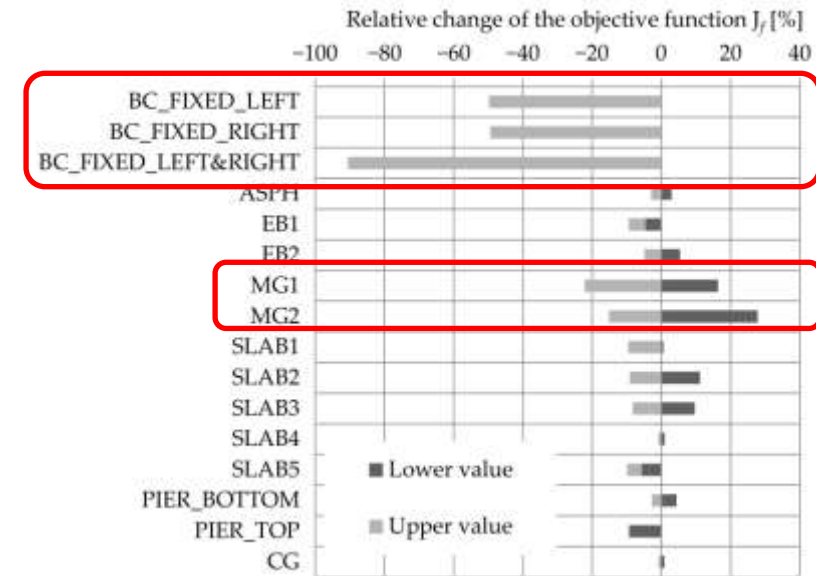
– Strain influence line

$$J_{IL} = RMSE = \sqrt{\frac{\sum_{j=1}^m (IL_{num,j} - IL_{exp,j})^2}{m}}$$

- The following properties/elements are the most sensitive:

– Boundary conditions (abutments's bearings)

Main girder 1 (MG1), main girder 2 (MG2)

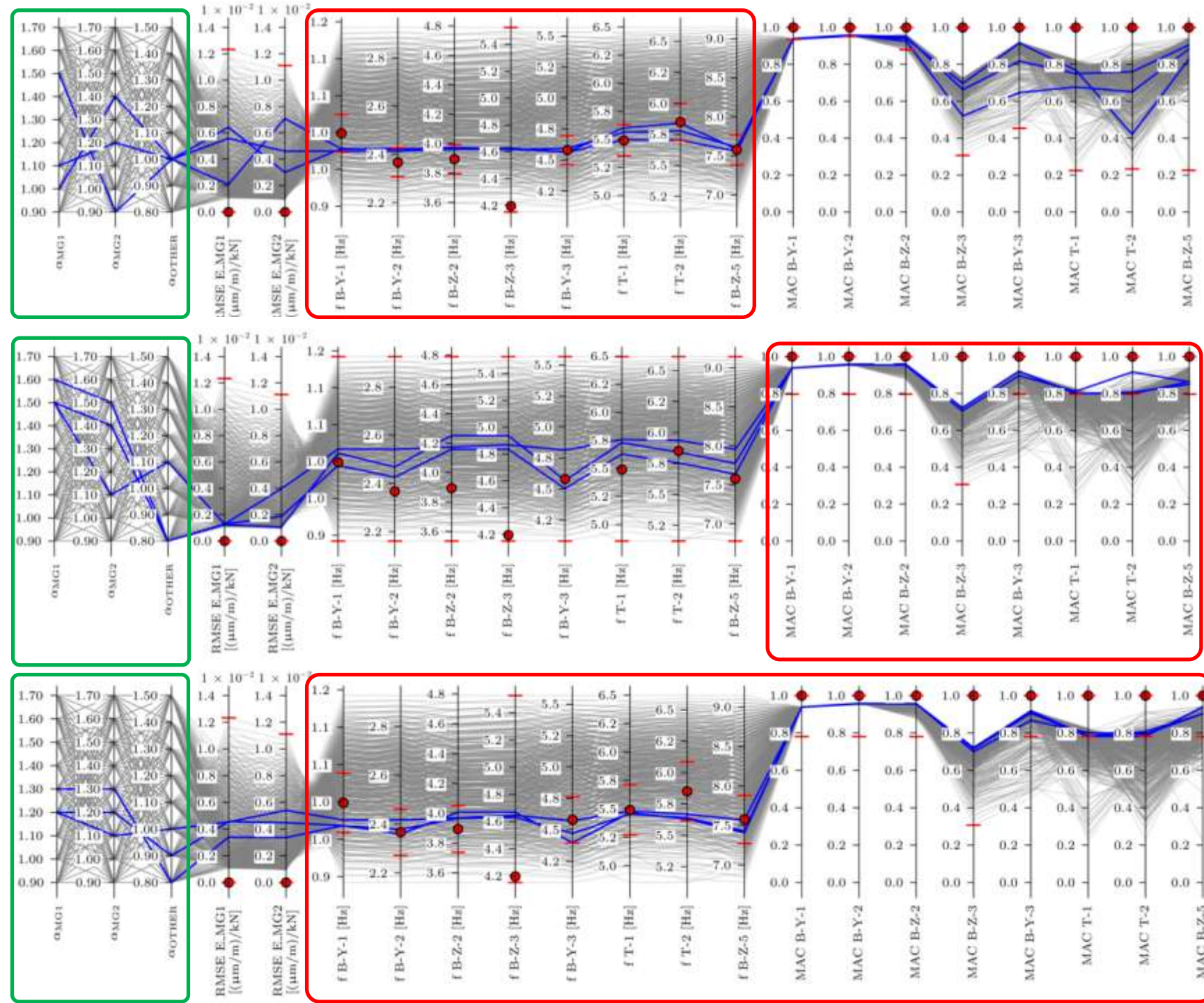


List of performed studies (4 + validation)

- Frequency-based EDMF
 - Only natural frequencies are considered
- MAC-based EDMF
 - Only mode shapes are considered
- Frequency & MAC-based EDMF
 - Both frequencies and mode shapes are considered
- Strain IL-based EDMF
 - Influence line is considered
- Validation
 - Validation is performed for the acceleration-based (frequency and MAC-based EDMF) and for the strain IL-based EDMF

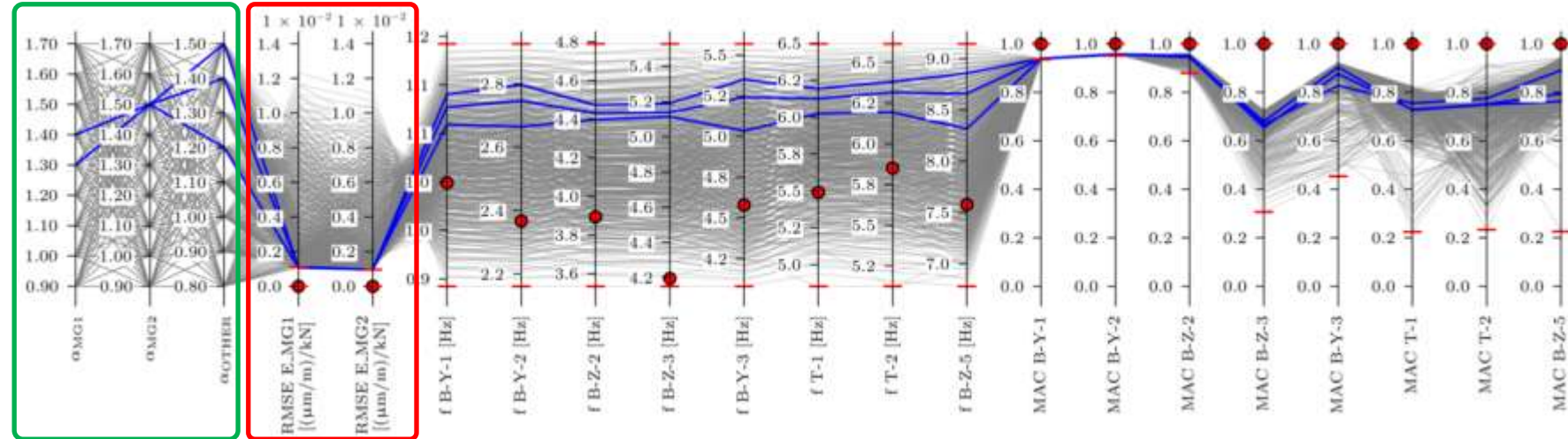
EDMF results

- Frequency-based EDMF results are consistent with the 2nd PhD paper (high α_{IM}^G and low α_{EMG} and vice-versa),
→ not engineeringly expected
- MAC-based EDMF gives very high values of both α_{MG1} and α_{MG2}
→ not engineeringly expected
- Combination of frequency and MAC-based EDMF gives the best sensible



Strain IL-based EDMF and comparison of EDMF results

- Frequency-based EDMF primarily improved the frequency values; a minor improvement was also seen for E-MG1 and E-MG2 strain ILs. The MAC values decreased.
- MAC-based improved MAC values, improvement in E-MG1 and E-MG2 strain ILs was greater than that in the frequency-based EDMF.
- Frequency and MAC-based EDMF improved frequencies and MACs, closely matching the results of frequency-based EDMF (for frequencies) and MAC-based EDMF (for MAC values), while both strain ILs did not align more closely with the measured ones.



FEMU Results	α_{MG1}	α_{MG2}	α_{OTHER}
Initial FE model	1.0	1.0	1.0
Frequency-based	1.0–1.5	0.9–1.4	1.0
MAC-based	1.5–1.6	1.1–1.5	0.8–1.1
Frequency and MAC-based	1.2–1.3	1.1–1.3	0.8–1.0
Strain IL-based	1.3–1.4	1.5	1.2–1.5

- Strain-based EDMF only improved both strain ILs

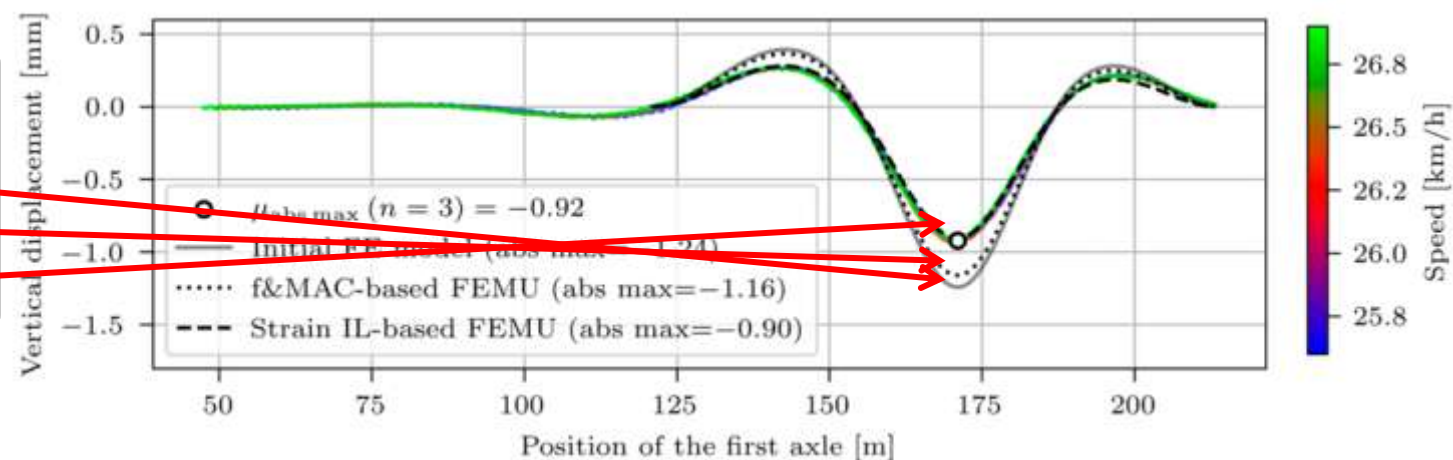
Validation (example for main girder 2)

D-MG2 mid-span vertical displacements under passage of calibration vehicle V2 -F



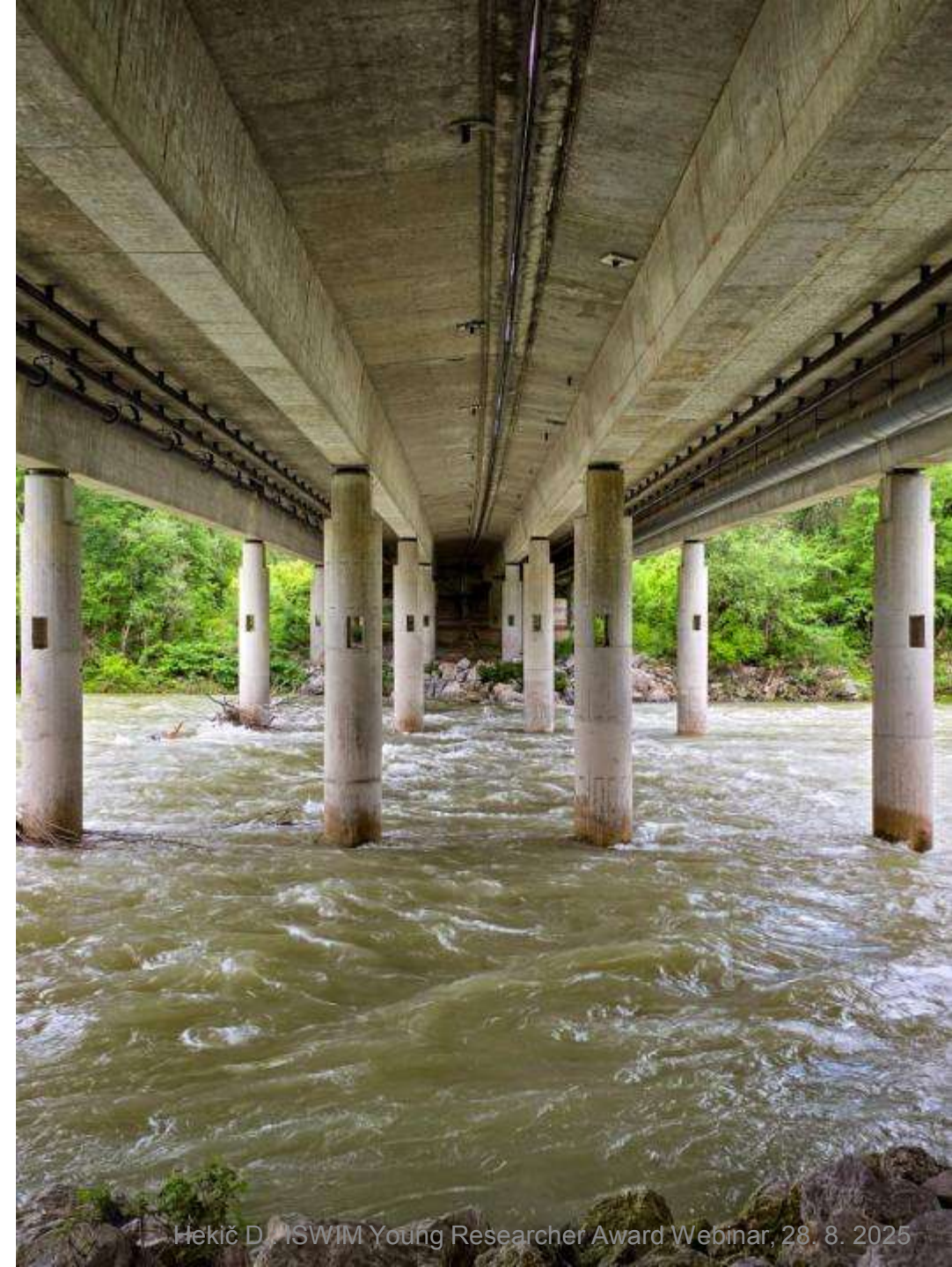
Max. response overestimation:

- Initial FE model: 35%
- Freq & MAC-based EDMF: 25%
- Strain-based IL EDMF: -2%



Conclusions

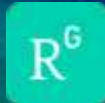
- Extensive experimental campaign, capturing **strains under calibration vehicles and ambient&traffic induced vibrations.**
- **Upgrading the ZAG's influence line** from normalised to absolute definition, investigating its load and speed dependence.
- **4 separate FEMU studies** to investigate the strain IL-based with the more common, acceleration-based FEMU results.
- **Validation** of the updated FE model with **independently measured vertical displacements.**
- **Relying solely on automatic FEMU,** without prior manual refinement, **can lead to misleading parameter estimates** due to unaccounted non-structural elements or incorrect boundary conditions.
- B-WIM extracted strain IIs can be used for FEMU
- **Strain IL-based FEMU results better matches with the measured displacements** and strains under calibration vehicles **than acceleration-based**
- **Bending stiffness** of the case study viaducts is **≈30% higher than designed.**
- Importance of aligning the measurement types with the intended model application: **acceleration data for dynamic behaviour** and **strain data for strain or displacement responses (safety analyses).**
- The thesis represents **step forward in bringing B-WIM systems closer to SHM**



Thank you for your attention!



doronhekić



Doron_Hekic

ZAG

ZAVOD ZA
GRADBENIŠTVO
SLOVENIJE

SLOVENIAN
NATIONAL BUILDING
AND CIVIL ENGINEERING
INSTITUTE



UNIVERSITY
OF LJUBLJANA

FGG

Faculty of Civil and
Geodetic Engineering

C STEL



DEWESoft
measurement innovation